

# A Ferrofluidic Magnetic Micropump

Anson Hatch, Andrew Evan Kamholz, Gary Holman, Paul Yager, and Karl F. Böhringer, *Member, IEEE*

**Abstract**—A microfluidic pump is described that uses magnetic actuation to push fluid through a microchannel. Operation relies on the use of magnetically-actuated plugs of ferrofluid, a suspension of nanosize ferromagnetic particles. The ferrofluid contacts but is immiscible with the pumped fluid. The prototype circular design demonstrates continuous pumping by regenerating a translating ferrofluidic plug at the conclusion of each pumping cycle. The flow rate can be controlled by adjusting device dimensions or the velocity of an external permanent magnet that directs the motion of the ferrofluid. The ferrofluidic plugs also serve as valves; if the magnetic actuator is stopped, pressure can be maintained with no power consumption. Flow can also be reversed by switching the direction of actuation. The maximum flow rate achieved with minimal backpressure was 45.8  $\mu\text{l}/\text{min}$ . The maximum pressure head achieved was 135 mm water (1.2 kPa). [558]

**Index Terms**—Ferrofluid, ferromagnetic, MEMS, microfluidic, micropump, microvalve.

## I. INTRODUCTION

MINIATURIZING fluid handling, chemical reactions, and chemical analysis to develop “lab on a chip” (LOC) technology has been an area of intense research over the last decade [1], [2]. A completely miniaturized and integrated system is expected to achieve portable chemical analysis, reduced error, reduced cost, and higher throughput. Effective LOC technology would greatly enhance genomic and proteomic research and improve medical treatment and environmental monitoring by introducing portable analytical systems. Manipulating microscale volumes of fluids is a vital component of LOC systems [1], [2]. Although several different micropumping mechanisms have been realized using a variety of actuation methods, it is not straightforward to integrate a micropump with other microfluidic components to create a LOC [2]. Micropumps have not generally been used to develop LOC systems due to limitations in the effectiveness of micropumps and the difficulty of combining or interfacing complex micropump fabrication schemes with the additional components of the system.

Existing micropumps vary in complexity and effectiveness. Diaphragm pumps have been presented that are actuated piezoelectrically [3]–[6], thermally [7], [8], pneumatically [8]–[10], and electrostatically [11], [12]. Diaphragm pumps have limi-

tations that include pulsatile flow and generation of air bubbles. Piezoelectric and electrostatic actuation require high voltages. Thermal actuation may degrade biological fluids by denaturing proteins. Diaphragm pumps also require valving mechanisms to direct flow. Valves with moving parts are susceptible to clogging by particles. Valves with no moving parts have also been realized [13]–[16] but are less efficient and remain open to reverse flow when pumping action is halted. Electrohydrodynamic pumps including ion drag [17], [18] and electroosmotic pumping used for capillary electrophoresis applications [19], [20] require high voltages and are highly sensitive to buffer conditions. It is highly desirable to achieve a simple yet effective micropump that could easily be combined with other microfluidic elements, particularly for analysis systems that are driven by the need for portability.

In this study, a novel and very simple microfluidic pumping mechanism is presented. A prototype pump is described that uses magnetically actuated plugs of ferrofluid for both pumping and valving. Since a liquid provides both the valving and pumping, the device does not require microfabricated moving parts and can be easily fabricated in silicon or other materials. This pumping mechanism should be simple to combine with microanalysis schemes even as part of an inexpensive disposable cartridge. It also has the potential of overcoming drawbacks that limit the effectiveness of other micropumps including particle loading, pumping of liquids and/or gasses, bubble tolerance, and sensitivity to solution buffering. Furthermore, when the power is removed, the pump stops flow in the presence of backpressure. The main purposes of this work were to demonstrate the simple principle of pumping by use of ferrofluidic plugs and to evaluate the use of a regenerative loop configuration for continuous pumping.

## II. THEORY AND DESIGN

The pumping mechanism relies on magnetic actuation to move a ferrofluidic plug that pushes and/or pulls the fluid of interest (Fig. 1). A ferrofluid contains nanosize ferromagnetic particles suspended in either an aqueous or an oil-based solvent [21]. Ferrofluids have been extensively studied and previously applied as an actuation mechanism [22]. A magnetically actuated ferrofluidic micropipette has been developed [23] and the movements of a polymeric ferrofluid gel have been proposed as an actuation mechanism for controlled delivery systems [24]. For this pumping application, the ferrofluid must be immiscible with the fluid being pumped; a hydrocarbon-based ferrofluidic suspension was tested for pumping water. The ferrofluid was retained in the pump chamber during operation, while the fluid of interest was pumped through the device with either forward or reverse flow.

Manuscript received March 31, 2000; revised February 15, 2001. The work of A. Hatch, A. E. Kamholz, G. Holman, and P. Yager was supported in part by DARPA under Contract N660001-97-C-8632. Subject Editor C.-J. Kim.

A. Hatch, A. E. Kamholz, and P. Yager are with the Department of Bioengineering, University of Washington, Seattle WA 98195 USA (e-mail: ahatch@u.washington.edu, kamholz@u.washington.edu, yagerp@u.washington.edu).

G. Holman is with the Washington Technology Center, Seattle, WA 98195 USA (e-mail: holman@cs.washington.edu).

K. F. Böhringer is with the Department of Electrical Engineering, University of Washington, Seattle, WA 98195 USA (e-mail: karl@ee.washington.edu).

Publisher Item Identifier S 1057-7157(01)04253-6.

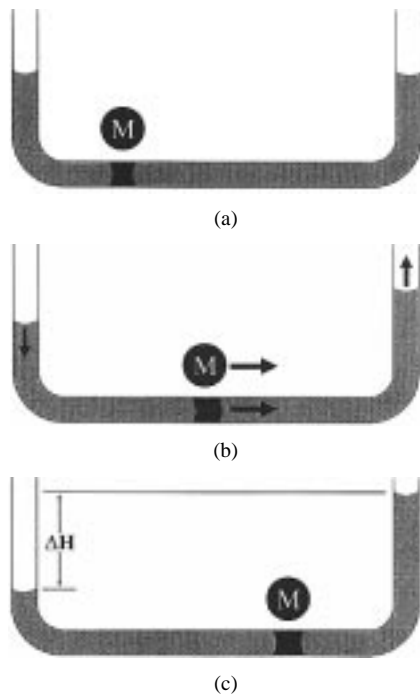


Fig. 1. Conceptual rendering of the use of ferrofluid as both a bistable valve and a fluid actuator. The lighter color fluid is the pumped fluid while the darker fluid is the ferrofluid. A permanent magnet (M) can be moved by external means. (a) The magnet is stationary and there is no pressure gradient between the inlet and outlet. (b) The magnet is moved to the right and the ferrofluid follows, actuating motion of the fluid to the right against an increasing hydrostatic pressure gradient. (c) The magnet is again stationary and the ferrofluid acts as a valve, withstanding the hydrostatic pressure gradient associated with the column of pumped fluid of height  $\Delta H$ . It is noteworthy that both valve states require no power, as the static permanent magnet is sufficient to maintain the position of the ferrofluid.

A closed-loop configuration was chosen for continuous pumping (Fig. 2). A circular geometry was used for easy implementation of the moving magnetic actuator. In this configuration, the ferrofluid acts as both a valve and a piston. A ferrofluidic valve, held in place by a stationary magnet, is always present in the short section of channel between the inlet and outlet of the pumping loop. A ferrofluidic plug serving as a piston is drawn around the channel by a translating magnetic field, in this case generated by an external permanent magnet attached to the rotor of a small electric motor. As the mobile plug is drawn around the pumping loop, fluid is drawn into the pumping loop through the inlet, and forced out through the outlet. If the mobile plug is stopped, it also serves as a valve, and if reversed, the direction of flow through the pumping loop reverses.

When the ferrofluid is exposed to the field gradient of an external magnet, it responds as a pool of magnetic liquid moving to the region of highest field. The forces that hold the ferrofluid in place are proportional to the gradient of the external field and the saturation magnetization value of the ferrofluid. The saturation magnetization value of the ferrofluid depends on the volume and is in the range of 100–900 G for a light oil suspension (125 G for the ferrofluid tested in the micropump).

As the cross-sectional area of the pumping loop is increased, leakage is more likely for a given magnetic field, because the ferrofluid must form a plug over a larger volume. However, as

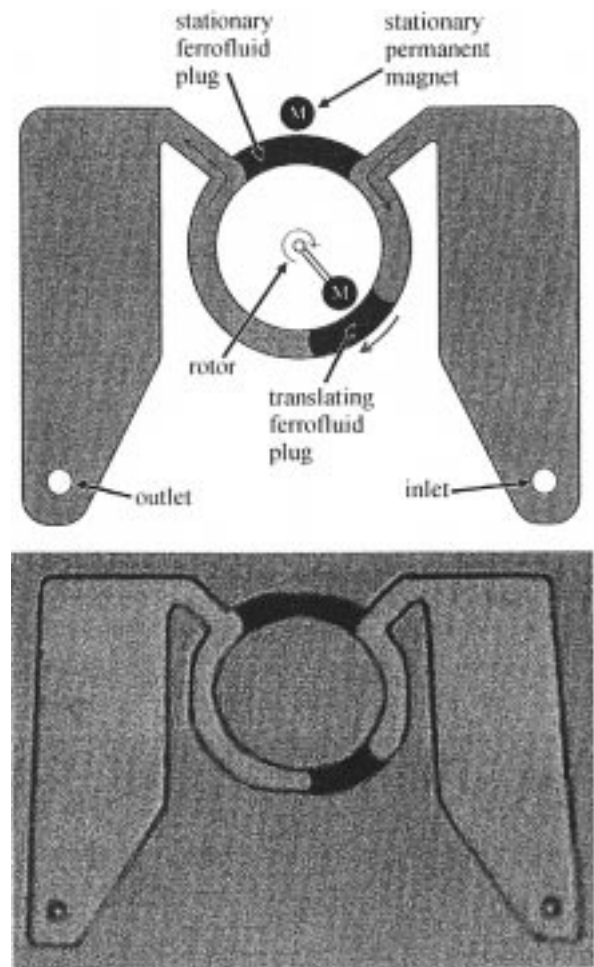


Fig. 2. Top: Schematic of the operating principle for the circular ferrofluidic pump. One plug of ferrofluid, held in place by a stationary magnet (M), acts as a closed valve between the inlet and outlet chambers. A second plug translates through the channel, pulling fluid in the inlet and pushing it out the outlet. The rotor is controlled by an external motor. Bottom: Optical micrograph of an actual device. Not shown are the permanent magnets used during operation. For scale, the inlet and outlet ports have a diameter of 1 mm.

the cross-sectional area is reduced, the channel imposes more resistance to fluid flow and to maintain an equivalent volumetric flow rate, the plug velocity must be increased. The maximum flow rate and pressure that can be generated are both dependent on the fluidic resistance of the channel. For fully developed incompressible laminar flow in a rectangular duct, the pressure gradient is expressed by [25]

$$\frac{dp}{dx} = 8 \frac{\mu Q (a+b)^2}{a^3 b^3} \quad (1)$$

where

- $Q$  volumetric flow rate;
- $\mu$  dynamic viscosity;
- $a$  and  $b$  short and long dimensions, respectively, of the cross section of the channel.

A ferrofluidic plug will follow the path of the moving magnetic field as long as the net force generated by the magnetic field acting on the ferrofluid is greater than the force imposed by the pressure gradient. Typical dimensions of  $a$  for microfluidic channels are 10  $\mu\text{m}$  to 1 mm, and typical flow rates are 1 nL/s

to 10  $\mu\text{L/s}$ . The viscosity of the ferrofluid used ( $\mu_{\text{ferrofluid}} = 9 \times 10^{-2} \text{ kg/m} \cdot \text{s}$  @ 25 °C) was 100 fold higher than for water ( $\mu_{\text{water}} = 9 \times 10^{-4} \text{ kg/m} \cdot \text{s}$  @ 25 °C). A relatively large cross-sectional area for the pumping loop (250  $\mu\text{m}$  etch depth by 2 mm channel width) was chosen in order to minimize resistance of the fluid channel. The pressure gradient that would develop in a straight channel with these dimensions, with  $Q = 1 \mu\text{L/s}$ , is  $dp/dx = 0.29 \text{ Pa/mm}$  for water and  $dp/dx = 29 \text{ Pa/mm}$  for ferrofluid. To achieve greater flow rates, either the rate of translation of the ferrofluidic plug must be increased or the etch depth of the channel must be increased. Both are limited by the ability of the permanent magnet to remain coupled with the ferrofluid. In the former case, the pressure gradient increases with flow rate, increasing the required electromagnetic force, while in the latter case, the magnet must act over a larger distance to hold the ferrofluid.

A closed-loop configuration allows continuous pumping with a regeneration phase; combining the moving and stationary ferrofluidic plugs at the end of each pump cycle and then separating a new translating plug from the mixture (Fig. 3). When the translating magnet approaches the region of the stationary magnet, the ferrofluid is exposed to the combined magnetic field of both magnets. The ferrofluidic plugs merge and respond as a single dynamic fluidic plug that shifts as the translating magnet passes by the stationary magnet. When the translating magnet begins a new pump cycle and moves away from the region of the stationary magnet, a portion of the ferrofluid is more strongly affected by the field of the translating magnet and separates to form a new translating ferrofluidic plug. An outer diameter for the pumping loop of 1 cm was chosen to allow the two external magnets to localize the field to desired regions of the pumping loop.

For this design, it is important that enough ferrofluid is introduced into the channel to entirely block the inlet or outlet of the pumping loop at all times during the regeneration phase, or the pressure difference across the loop will induce backflow. If the pumped fluid wets the channel surface much more readily than the ferrofluid, leakage between the channel wall and the ferrofluidic plug is possible.

### III. FABRICATION AND ASSEMBLY

Pump fabrication employed traditional photolithographic techniques that have been discussed elsewhere [26]. Briefly, the pump design was printed on a transparent film and mounted on a glass plate to act as a mask. A test-grade 4-in (100) silicon substrate ( $\sim 430 \mu\text{m}$  thick, International Wafer Service, PortolaValley, CA) was oxidized and coated with AZ1512 positive photoresist (Clariant Corporation, Somerville, NJ). After UV lithography, the resist was removed, and silicon dioxide was removed using a hydrofluoric acid etchant (BOE) with the patterned resist functioning as a mask. The exposed silicon was etched using EDP (ethylenediamine, pyrocatechol, and water). The inlet and outlet ports were drilled using a diamond-tipped drill bit (TSI Inc., Seattle, WA) in a rotary tool (Dremel, Racine, WI). A borosilicate wafer ( $\sim 290 \mu\text{m}$  thick, U.S. Precision Glass, Elgin, IL) was anodically bonded to the

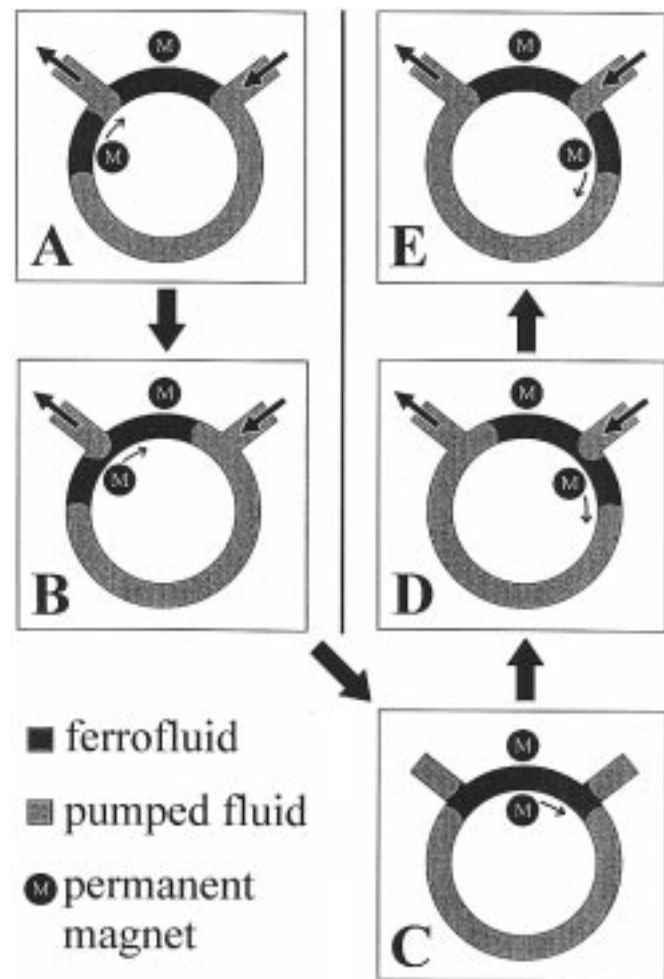


Fig. 3. Conceptual rendering of the regenerative phase of pump operation. In part A, the translating plug approaches the pumping loop outlet as net flow continues through the loop. Part B shows the merging of the translating and stationary ferrofluidic plugs. In part C, the plugs are fully merged. There is no net flow and the inlet and outlet legs are blocked, preventing leakage. Part D shows the regeneration of the translating plug as the revolving magnet moves away from the stationary magnet. Net flow begins again at this time. In part E, the newly formed plug proceeds along the pumping loop.

silicon to enclose the channels. Finally, the bonded wafer was diced to produce five identical devices.

Following fabrication, blunt, 18-gauge needles were affixed over the fluidic access holes using epoxy to provide an interface to 18-gauge teflon tubing (Small Parts Inc., Miami Lakes, FL). Permanent “bullet” magnets (neodymium composite, 6 mm diameter, 3 mm thick, surface Gauss = 3500, Restoration Hardware, Corte Madera, CA) were used as both the stationary and revolving magnetic field sources. The stationary magnet was affixed to the glass side of the device using epoxy. The revolving magnet was similarly affixed to an aluminum rotor, which was attached to a dc motor (#V41-865, Edmund Scientific, Barrington, NJ) that was powered with a variable 3–14 V dc external power supply (BK Precision, Chicago, IL). The rotating magnet assembly was visually aligned with the pumping loop and clamped in place. Devices were first filled with water. Ferrofluid (APG E18, temperature of boiling and decomposition  $> 200 \text{ }^\circ\text{C}$ , Ferrofluidics Corporation, Nashua, NH) was then loaded by introducing a pool of ferrofluid at one of the ports with

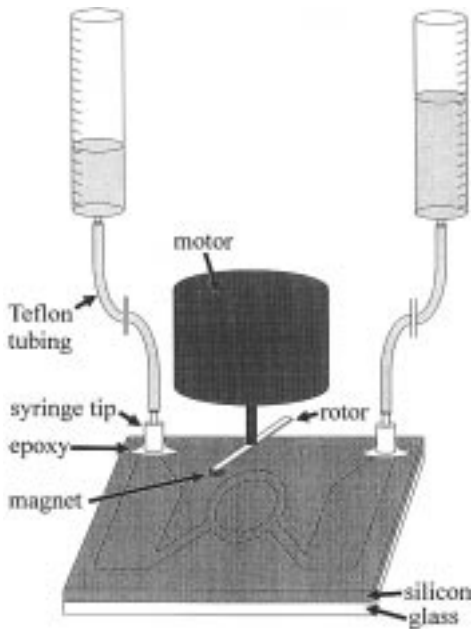


Fig. 4. Schematic of the experimental setup. The device rests face down. Syringe tips are attached to both the inlet and outlet holes to act as fluid interconnects. Each tip is connected to a fluid column by flexible tubing. The motor is placed over the device so that the revolving magnet moves over the pumping loop (location shown with dotted lines). During operation, the motor is much closer to the device, with the magnet riding just off the silicon surface (about 1 mm away). Not shown are various clamps used to hold the device, motor, and columns.

a syringe and manually moving it into position with a handheld permanent magnet. Once the ferrofluid pool entered the inlet of the pumping loop, the permanent magnets used for pump operation rapidly forced the ferrofluid into the desired locations during operation. Loading slight excess was not problematic, as the pumping operation tended to expel excess ferrofluid from the main pumping loop.

#### IV. MEASUREMENTS

The experimental setup is shown in Fig. 4. The magnets were oriented with the same polarity, which was perpendicular to the plane of the device. The moving permanent magnet revolved on the underside of the device, directly under the pumping loop. Columns of water were attached to both the inlet and outlet, with care taken not to trap air bubbles in the system. The columns and tubing connecting the device, having dimensions much wider than the device channels, contributed negligible resistance to system flow. Initially, both columns of water were at the same height. The motor was continuously run at a particular speed, first in a clockwise direction (from the perspective of motion of the ferrofluid plug in the pumping loop). The difference in height of the columns of water was recorded each minute until a steady-state height was reached. From the collected data, the flow rate (determined by the volume displaced in the columns) as a function of hydrostatic pressure was calculated (Fig. 5).

Once a steady-state height was reached, the direction of the motor was reversed. This resulted initially in a very high flow rate due to the hydrostatic pressure gradient in the flow direction generated from the first phase of the experiment. After reaching

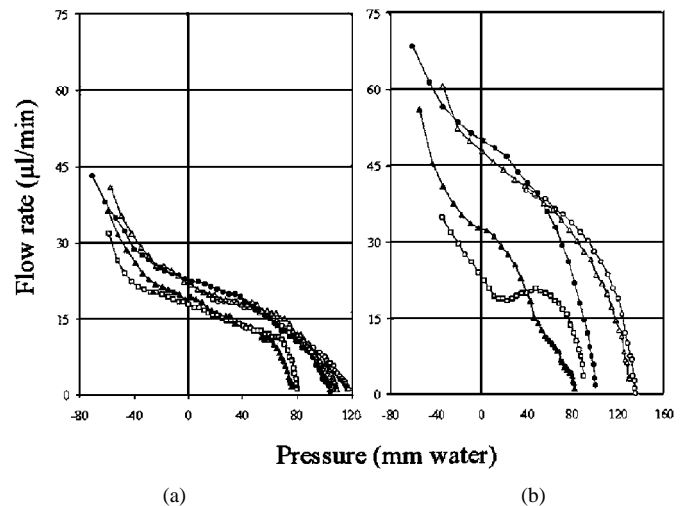


Fig. 5. Measurements of flow rate vs. pressure for studies with motor speed of (a) 4 rpm and (b) 8 rpm. For both plots: day 1 first clockwise (CW) trial ( $\circ$ ), day 1 first counterclockwise (CCW) trial ( $\bullet$ ), day 1 second CW trial ( $\triangle$ ), day 2 second CCW trial ( $\blacktriangle$ ), day 3 third CW trial ( $\square$ ). Pressure values were determined by the difference in height of the columns of water attached to the inlet and outlet. Positive pressure values indicate a gradient against the flow direction while negative pressure values indicate a gradient with the flow direction. The negative values occur when the motor direction is switched from one trial to the next.

a steady-state height while going counterclockwise, the direction was again reversed. After making measurements, the pump was then left running overnight and was switched back to counterclockwise after one day. Measurements continued into a third day when the motor was again run clockwise. This 3-day study was completed for motor speeds of 4 and 8 rpm for totals of over 17 000 and 34 000 revolutions respectively. Motor speeds greater than 8 rpm generated pressure gradients too large for maintaining coupling between the permanent magnet and the translating ferrofluidic plug. The purpose of making measurements on the later days was to study degradation of the ferrofluid over time. This was monitored by comparing the maximum achievable pressure for multiple runs in the same direction. These results are summarized in Table I. It was consistently found that performance in the counterclockwise direction was not as good as in the clockwise direction, as the second clockwise trial always produced a higher steady-state pressure than the first counterclockwise trial; attributed to nonuniform alignment of the translating magnet with the pumping loop.

For clarity, backflow through the device will be referred to as either "static" or "dynamic" leakage. Static leakage describes backflow resulting from failure of a stationary ferrofluidic plug to seal the channel against a pressure gradient. A static leakage test was performed by stopping the motor when the plugs were in the approximate positions shown in Fig. 2(a). In this orientation, the flow between the inlet and outlet should be completely blocked by the two plugs. Water was added in small increments ( $\sim 5$  mm every five minutes) to the outlet column in order to increase the applied pressure. No leakage was seen for pressures up to 200 mm of water. At pressures over 200 mm of water, the ferrofluidic plug (the plug that translates during pumping mode) was no longer held in place by the force of the magnetic field due to the force of the pressure gradient, and sudden dramatic leakage occurred. A long-term test was performed at 150 mm

TABLE I  
PUMP PERFORMANCE DURING CONTINUOUS OPERATION

	4 RPM		8 RPM	
	Time <sup>1</sup>	Decrease <sup>2</sup>	Time <sup>1</sup>	Decrease <sup>2</sup>
First clockwise trial (day 1) vs. second clockwise trial (day 1)	2 hr	7%	1 hr	4%
First counterclockwise trial (day 1) vs. second counterclockwise trial (day 3)	1 day	27%	1 day	18%
First clockwise trial (day 1) vs. third clockwise trial (day 3)	2 days	32%	2 days	34%

<sup>1</sup>Time elapsed between the two trials being compared

<sup>2</sup>Percent decrease in the steady-state pressure gradient developed between the two trials

of water, with no observable leakage over a period of one week. This was true even for ferrofluid that had been run for several days in pumping mode, indicating that the maximum pressures achieved and losses in pressure over increasing flow rates is due to a dynamic leaking process.

The flow curves in Fig. 5 are approximately linear over the –20 to 40 mm pressure range for slower flow rates (4 rpm). This indicates that leakage is mainly in direct proportion to the hydrostatic pressure. The leakage probably occurred during the regenerative phase while the revolving magnet was directly adjacent to the stationary magnet and all of the ferrofluid was pooled in the same location (refer to Fig. 3(C)). Some backflow of water occurred through the longer path between the inlet and outlet by displacement at the edges of the pooled ferrofluid. This dynamic leakage is more pronounced in the nonlinear portions of the flow curves (at high pressures, both positive and negative) as the ferrofluid is displaced for a longer duration. This leaking mechanism was verified optically during the experiments. It is apparent that dynamic leakage is worse at higher pressures, as evidenced by the larger linear ranges of the measurements at slow flow rates.

To evaluate the pump, it is useful to compare the measured flow rate with the expected flow rate, based on the volume of the pumping loop and the rate of revolution of the motor. With an approximate outer diameter of 1.1 cm, approximate inner diameter of 0.9 cm, and an etch depth of 0.025 cm (250  $\mu\text{m}$ ), the volume of the pumping loop was about 7.9  $\mu\text{l}$ . About one fourth of this space was filled with ferrofluid that reduces the effective volume of the pumping loop. Therefore, at a motor speed of 4 rpm, the expected volumetric flow rate is 24  $\mu\text{l}/\text{min}$ .

For measurements of flow rate with minimal backpressure (extrapolated from measurements of flow rate when differences in column heights was close to zero), the flow rate on day 1 in the clockwise direction was 22.5  $\mu\text{l}/\text{min}$ , which is in good agreement with the predicted value. Similarly, the predicted flow rate at 8 rpm is 48  $\mu\text{l}/\text{min}$ , which compares favorably with the measured value of 47.8  $\mu\text{l}/\text{min}$ . The similarity between predicted and measured flow rates with minimal backpressure indicates that fluid actuation by a ferrofluidic plug is very efficient, since no significant leakage was detected. In addition, the static leakage test demonstrated that no water slipped past the ferrofluid plugs over the entire pressure range used in this study. These results suggest that the surface energies of the ferrofluid and water are appropriate for the silicon and glass device used

in this study; this pump was efficient because the device surfaces were readily wetted by the ferrofluid. A thin coating of ferrofluid was also observed on the channel walls of the device; which although undesirable, may be unavoidable in order to minimize leaking. Throughout experimentation, ferrofluid was only observed in regions of the device where ferrofluidic plugs had directly contacted the device walls. No visual traces were detected in the tubing or columns used for measuring the pressure gradient. The fluid of interest need not be pumped directly through the device, as a buffer could be displaced by the pump and coupled downstream to the fluid of interest. Via this mechanism, concerns of sample contamination through contact with the ferrofluid can be eliminated.

Over the course of each 3-day experiment, the ferrofluid changed from near-black to brown and tended to coat the channel surfaces in spots rather than flow in one smooth plug. These changes in properties suggest degradation of the ferrofluid and changes in the surface chemistry of the channel walls, paralleling the decrease in flow rate on days 2 and 3 of each experiment. The drop in flow rates appears to be a result of changes in dynamic leakage as the static leakage test was unaffected by this change.

Additional tests were performed to calculate the dynamic properties of the pump over a single cycle of operation. For this purpose, fluorescent microspheres (1  $\mu\text{m}$  diameter; Polysciences, Inc., Warrington, PA) were loaded into the fluid being pumped. The velocities of fluorescent microspheres were measured during pump operation as an indication of flow rate. Images of the fluorescent particles were captured in the inlet leg with a CCD camera (Optronics DEI-750, Goleta, CA) mounted on an epi-illuminated fluorescence microscope (Zeiss, Thornwood, NY) at 10 $\times$  magnification. The normalized flow rates inferred by particle velocities are plotted in Fig. 6 for a single pump cycle at 4 RPM.

As plotted in Fig. 6, the cycle begins (Phase A) as the rotating ferrofluid plug is beginning to form near the inlet [transition of Fig. 3(C)–(D)]. The flow rate gradually increases as the plug separates from the ferrofluid pool and the ferrofluid near the permanent magnet remains in place. Through Phase B of the cycle, the moving ferrofluid plug is traversing the bulk of the pump loop [transition of Fig. 3(E)–(A)]. The velocity was nearly constant during this phase. Flow through the inlet reaches a maximum and then rapidly drops during Phase C of the cycle as the moving plug nears the outlet leg of the pump loop [tran-

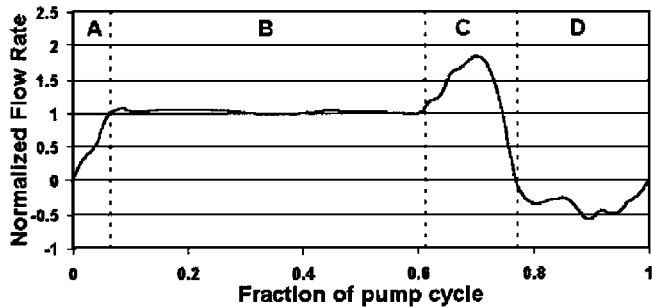


Fig. 6. Measurements of flow rate during the pumping cycle. Flow rates were inferred by tracking the velocity of fluorescent microspheres at the inlet leg of the pumping loop during operation at 4 RPM with minimal backpressure. The plot shows a normalized flow rate adjusted such that the relatively constant velocity observed during phase B averaged to a value of 1 corresponding to the moving ferrofluidic plug traversing the bulk of the open channel between the inlet and outlet legs of the channel. The  $x$ -axis represents the fraction of the pumping loop traversed during one cycle. Other phases correspond to: the initial formation of the translating plug separating from the stationary plug (Phase A), merging of the translating plug with the stationary plug (Phase C), and movement of the rotating magnet over the stationary plug (Phase D) (see text for more complete description). The data is based on an average of data collected during several cycles of operation.

sition of Fig. 3(A)–(B)]. During this phase, the rotating magnet attracts some ferrofluid of the stationary plug toward the moving plug accelerating flow until the outlet leg is blocked and the ferrofluid begins moving toward the inlet leg. At this point in the cycle, Phase D, flow is reversed as ferrofluid is pushed back toward the inlet [transition of Fig. 3(B)–(C)]. Once the outlet leg is no longer blocked a new rotating ferrofluidic plug is formed and a new cycle begins.

## V. DISCUSSION

The experimental results demonstrate the feasibility of using magnetically-actuated ferrofluidic plugs as a means of pumping and valving fluids. The ferrofluid proved to be a robust means of actuation as it readily conformed to the geometry of a microchannel, and ferrofluidic plugs can easily be merged or separated. When working as a simple valve, the plugs were maintained at pressures greater than 1.7 kPa. The plugs could easily be manipulated through the channels at linear velocities up to 3.75 mm/s using a translating permanent magnet while generating pressures up to 1.2 kPa.

Many suitable fabrication techniques and materials could be used to make the simple structures necessary for this design. In addition to the Si-glass system used here, glass, laser-cut plastic laminate layers, and injection-molded plastic are possibilities. It is also possible to use an array of electromagnets that are fabricated directly on chip [27] to manipulate the ferrofluid as opposed to external magnets. However, current electromagnets would require more power than the electric motor used and would have to be continually powered to prevent backflow. At the highest operating speeds, the motor required 6.1 V and 1.9 mA ( $P = 11.6$  mW) where an electromagnet fabricated on a 2 mm  $\times$  3 mm device required 0.8 V and 500 mA ( $P = 40$  mW) to generate a field of 300 G [26].

In the current design, pumping action is halted during the plug regeneration phase of the cycle. A near-continuous flow rate may be achieved through the majority of one pump cycle provided

the channel is uniform in size and the translating plug is moved at uniform velocity. This was observed during phase B of the pump cycle shown in Fig. 6. If a continuous flow rate is necessary over longer time periods, there are at least two viable options. One is to make the pumping loop large enough to complete the necessary pumping within one cycle. A second option is to use multiple pumping loops matched out of phase, with one loop in regeneration mode at all times to provide a continuous flow rate.

## VI. CONCLUSION

The work demonstrates the feasibility of ferrofluidic plugs as fluid actuators for a microscale pump. Because of the ease of manufacture and low cost, this technology could be used in many different formats and is amenable to many other device geometries and materials. The biggest advantage of using a ferrofluid is that it can block the entire cross section of a fluid channel and adapt to changes in the shape of the channel. For the system studied here, significant degradation of the ferrofluid was seen after two days of continuous operation. For situations that require pumping for only short intervals, such a pump could be useful. There is also the possibility of further developing the constituent materials in order to prolong the properties of the ferrofluid and optimizing the design to extend the life of the ferrofluid and improve pumping performance.

The prototype pump was successful at pumping water at flow rates of 22.5  $\mu\text{l}/\text{min}$  and 45.8  $\mu\text{l}/\text{min}$  with minimal backpressure for motor velocities of 4 and 8 rpm, respectively. The maximum pressure generated was 117 and 135 mm water for motor velocities of 4 and 8 rpm. By changing the geometry of the device and the speed of the motor, precise control of flow rates is possible and much lower flow rates than those tested can be achieved. Although it may not be feasible to fully integrate this micropump on chip using microfabricated electromagnets, it should be straightforward and inexpensive to integrate a ferrofluidic pump as described with existing microfluidic analysis elements since the pump requires a simple channel for operation. An external magnet control system could be compact and consume very little power allowing the generation of a small LOC system with an integrated micropump.

## ACKNOWLEDGMENT

The authors wish to thank Ferrofluidics Corporation for providing the ferrofluid, H. S. Fuji, Manager of the Washington Technology Center Microfabrication Laboratory, for use of the microfabrication facility, and Micronics, Inc., Redmond, WA, for support; particularly from Dr. B. Weigl. They also thank R. R. L. Murillo for help with recording measurements and Dr. R. Bardell for insight regarding micropump performance and characterization. Most importantly, the authors would like to thank Dr. W. E. Lee from the Defence Research Establishment, Suffield, for considerable inspiration in working with ferrofluids.

## REFERENCES

- [1] G. H. W. Sanders and A. Manz, "Chip-based microsystems for genomic and proteomic analysis," *Trac-Trends in Analytic. Chem.*, vol. 19, pp. 364–378, 2000.

- [2] A. van den Berg and T. S. J. Lammerink, "Micro total analysis systems: Microfluidic aspects, integration concept and applications," in *Microsystem Technology in Chemistry and Life Science*, 1998, vol. 194, Topics in Current Chemistry, pp. 21–49.
- [3] H. Vanlintel, F. Vandepol, and S. Bouwstra, "A piezoelectric micropump based on micromachining of silicon," *Sensors Actuators*, vol. 15, pp. 153–167, 1988.
- [4] S. Kar, S. McWhorter, S. Ford, and S. Soper, "Piezoelectric mechanical pump with nanoliter per minute pulse-free flow delivery for pressure pumping in micro-channels," *Analyst*, vol. 123, pp. 1435–1441, 1998.
- [5] M. Koch, N. Harris, A. Evans, N. White, and A. Brunnschweiler, "A novel micromachined pump based on thick-film piezoelectric actuation," *Sensors Actuators*, vol. 70, pp. 98–103, 1998.
- [6] R. Linnemann, P. Woias, C. Senfft, and J. Ditterich, "A self-priming and bubble-tolerant piezoelectric silicon micropump for liquids and gases," in *Proc. MEMS 98. IEEE. Eleventh Annual International Workshop on Micro Electro Mechanical Systems. An Investigation of Micro Structures, Sensors, Actuators, Machines and System*, New York, NY, 1998.
- [7] W. Benard, H. Kahn, A. Heuer, and M. Huff, "Thin-film shape-memory alloy actuated micropumps," *J. Micromech. Syst.*, vol. 7, pp. 245–251, 1998.
- [8] F. Vandepol, H. Vanlintel, M. Elwenspoek, and J. Fluitman, "A thermopneumatic micropump based on micro-engineering techniques," *Sensors Actuators*, vol. 21, pp. 198–202, 1990.
- [9] J. Cunneen, Y. Lin, S. Caraffini, J. Boyd, P. Hesketh, S. Lunte, and G. Wilson, "A positive displacement micropump for microdialysis," *Mechatronics*, vol. 8, pp. 561–583, 1998.
- [10] R. Rapp, W. Schomburg, D. Maas, J. Schulz, and W. Stark, "LIGA micropump for gases and liquids," *Sensors Actuators*, vol. 40, pp. 57–61, 1994.
- [11] R. Zengerle, J. Ulrich, S. Kluge, M. Richter, and A. Richter, "A bidirectional silicon micropump," *Sensors Actuators*, vol. 50, pp. 81–86, 1995.
- [12] T. Bourouina, A. Bosseboeuf, and J. Grandchamp, "Design and simulation of an electrostatic micropump for drug-delivery applications," *J. Micromech. Microeng.*, vol. 7, pp. 186–188, 1997.
- [13] R. Bardell, N. Sharma, F. Forster, M. Afromowitz, and R. Penney, "Designing high-performance micro-pumps based on no-moving-parts valves," in *Proc. Microelectromechanical System (MEMS). The 1997 ASME International Mechanical Engineering Congress and Exposition*, New York, NY, USA, 1997.
- [14] A. Olsson, P. Enoksson, G. Stemme, and E. Stemme, "Micromachined flat-walled valveless diffuser pumps," *J. Microelectromech. Syst.*, vol. 6, pp. 161–166, 1997.
- [15] E. Stemme and G. Stemme, "A valveless diffuser/nozzle-based fluid pump," *Sensors Actuators*, vol. 39, pp. 159–167, 1993.
- [16] A. Olsson, O. Larsson, J. Holm, L. Lundbladh, O. Ohman, and G. Stemme, "Valve-less diffuser micropumps fabricated using thermoplastic replication," *Sensors Actuators*, vol. 64, pp. 63–68, 1998.
- [17] S. Ahn and Y. Kim, "Fabrication and experiment of a planar micro ion drag pump," *Sensors Actuators*, vol. 70, pp. 1–5, 1998.
- [18] A. Richter, A. Plettner, K. Hofmann, and H. Sandmaier, "A micromachined electrohydrodynamic (EHD) pump," *Sensors Actuators*, vol. 29, pp. 159–168, 1991.
- [19] S. Arulanandam and D. Li, "Liquid transport in rectangular microchannels by electroosmotic pumping," *Colloids Surf.*, vol. 161, pp. 89–102, 2000.
- [20] P. Fletcher, S. Haswell, and V. Paunov, "Theoretical considerations of chemical reactions in micro-reactors operating under electroosmotic and electrophoretic control," *Analyst*, vol. 124, pp. 1273–1282, 1999.
- [21] E. Dubois, V. Cabuil, F. Boue, and R. Perzynski, "Structural analogy between aqueous and oily magnetic fluids," *J. Chem. Phys.*, vol. 111, pp. 7147–7160, 1999.
- [22] H. Hartshorne, Y. Ning, W. E. Lee, and C. Backhouse, "Development of Microfabricated Valves for  $\mu$  TAS," in *Proc. Micro Total Analysis Systems '98*, Banff, Canada, 1998.
- [23] N. Greivell and B. Hannaford, "The design of a ferrofluid magnetic pipette," *IEEE Trans. Biomed. Eng.*, vol. 44, pp. 129–135, 1997.
- [24] M. Zrinyi, D. Szabo, and L. Barsi, "Magnetic field sensitive polymeric actuators," *J. Intell. Mat. Syst. Struct.*, vol. 9, pp. 667–671, 1998.
- [25] F. M. White, *Fluid Mechanics*, 3rd ed. New York, 1994.
- [26] J. P. Brody, A. E. Kamholz, and P. Yager, "Prominent Microscopic Effects in Microfabricated Fluidic Analysis Systems," in *Proc. Micro- and Nanofabricated Electro-Optical Mechanical Systems for Biomedical and Environmental Applications*, 1997, pp. 103–110.
- [27] C. Ahn, M. Allen, W. Trimmer, Y. Jun, and S. Erramilli, "A fully integrated micromachined magnetic particle separator," *J. Microelectromech. Syst.*, vol. 5, pp. 151–158, 1996.



**Anson Hatch** received the B.S. degree in biomedical engineering from Boston University, Boston, MA, in 1997. He is currently pursuing the Ph.D. degree in bioengineering at the University of Washington, Seattle, WA, studying diagnostic applications of microfluidics.

While at Boston University, he worked on solid phase DNA amplification and selection of DNA aptamers.



**Andrew Kamholz** is pursuing the Ph.D. degree in the Department of Bioengineering at the University of Washington, Seattle. He received the B.S. degree in biomedical engineering from the Johns Hopkins University, Baltimore, MD, in 1996. His graduate studies focus on diffusion, chemical reaction, and hydrodynamic phenomena in microfluidic systems.



**Gary Holman** received the B.S. degree in biochemistry from Western Washington University, WA, in 1997. He is pursuing the B.S. degree in computer science at the University of Washington, Seattle.

He is currently a Process Engineer at the Washington Technology Center, Seattle.



**Paul Yager** received the A.B. degree in biochemistry from Princeton University, Princeton, NJ, and the Ph.D. degree in chemistry from the University of Oregon, Eugene.

He is a Professor in the Department of Bioengineering at the University of Washington, Seattle, and since 1987, his primary focus has been development of sensing technology for use in biomedical diagnostics. His laboratory is now engaged in development of microfluidic analytical methods.



**Karl Böhlinger** (S'94–M'97) received the M.S. and Ph.D. degrees in computer science from Cornell University, Ithaca, and the Diplom-Informatiker degree from the University of Karlsruhe, Germany. His dissertation on design and control of microactuator arrays was performed at the Cornell Nanofabrication Facility and at the Stanford Transducers Laboratory. At the University of California at Berkeley, he investigated micro self-assembly techniques as a Postdoctoral Researcher.

He is an Assistant Professor in Electrical Engineering at the University of Washington, Seattle. His current interests include distributed MEMS, micromanipulation and microassembly, and MEMS bio-implants.

Dr. Böhlinger received an NSF Postdoctoral Associateship in 1997 and an NSF CAREER award in 1999.